



Hadronic Mono- W' Probe of Dark Matter at Colliders

Speaker: Kun Cheng (Peking University)

chengkun@pku.edu.cn

arXiv: 2311.13578

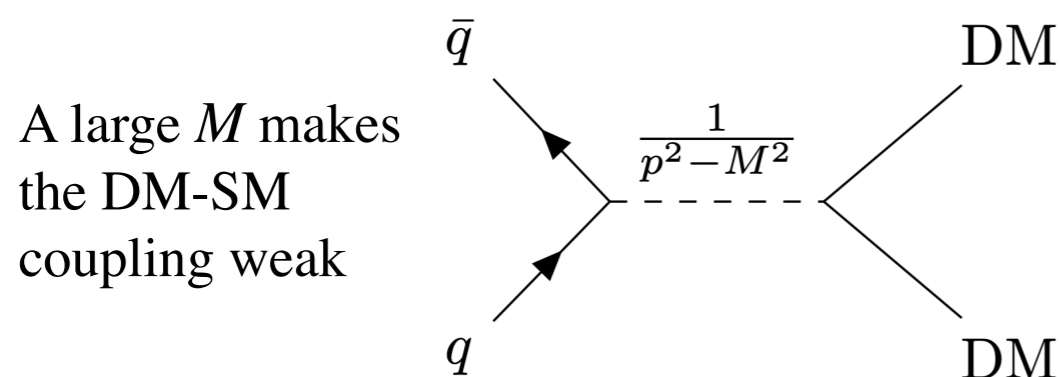
R. Holder, J. Reddick, M. Cremonesi, D. Berry,
K. Cheng, M. Low, T. Tait, D. Whiteson

Dark Matter search at Collider

Collider signal of DM: Visible + E_T (Mono- X)

DM interact with SM particles via EFT operator:

$g/q + E_T$: 1002.4137, 1108.1196, 1408.3583, 1502.01518...
$t/b + E_T$: 1303.6638, 1410.4031, 1503.00691
$\gamma + E_T$: 1109.4398, 1410.8812, 1411.1559
$W/Z + E_T$: 1309.4017, 1408.2745, 1404.005.....
$h + E_T$: 1312.2592, 1402.7074

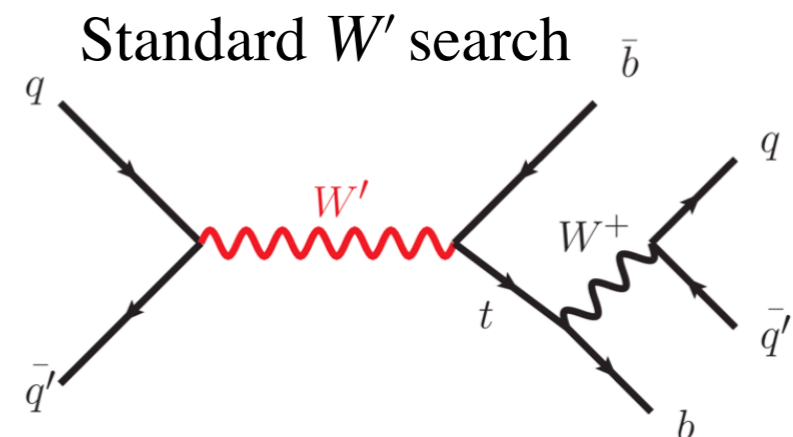


When the NP particles are produced on-shell decay to SM particles

$Z' + E_T$: 1504.01386

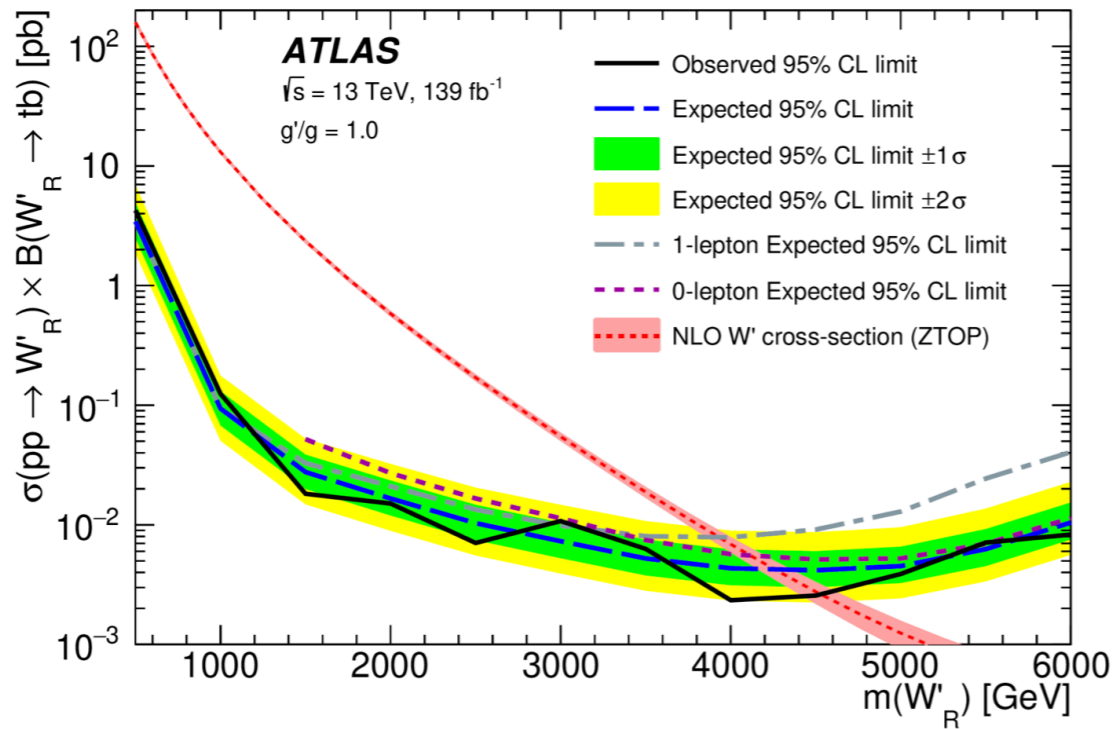
$W' + E_T$: This Work: $W' \rightarrow tb$

W' : similar interaction with the SM W boson:
 Resonant production
 Stringent Limits



Resonant production of W' with a dark Higgs boson

2308.08521

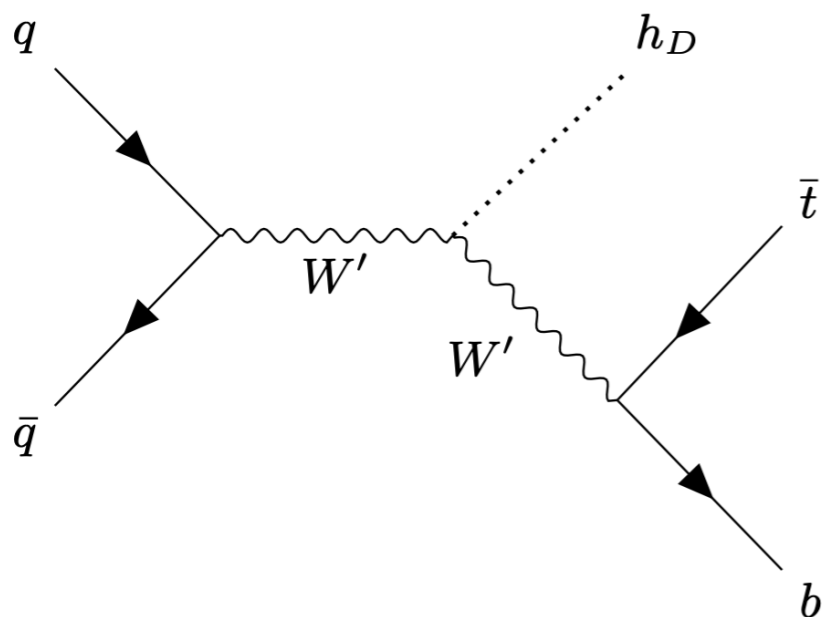


Stringent trigger requirement

$$p_T > 500 \text{ GeV}$$

Mass region smaller than 1 TeV are not probed

$W' + \text{DM}$ The channel we are using:



$m_{W'}$: focus on 250 ~ 1750 GeV

A dark Higgs is emitted from W'

$$\cancel{E}_T > 200 \text{ GeV}$$

In addition to the DM search, this channel opens up the possibility to push W' searches to lower masses

UV models with W' commonly have a dark Higgs boson

- W' comes from a new gauge symmetry that is broken before EWSB.

- There is new scalar responsible for the breaking:

$$\phi = h_D + v_\phi$$

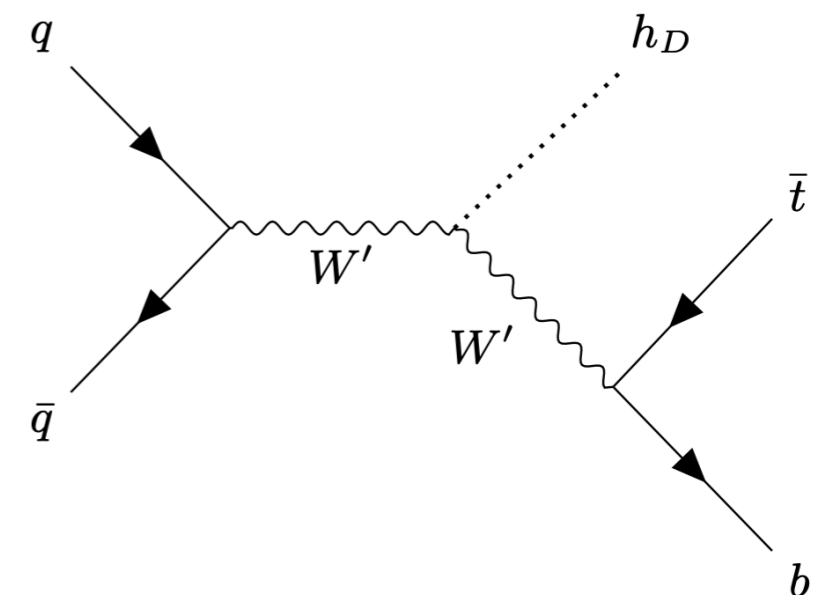
- The scalar gives W' mass, and couples to W' :

$$\propto g_{new} W'^2 (h_D + v_\phi)^2$$

Relevant Parameters

- masses: $m_{h_D}, m_{W'}$
- W' - t - b : new gauge coupling strength g_{new}
- W' - W' - h_D : new gauge coupling strength and W' mass ($m_{W'} \propto v_\phi$)

(nearly) model-independent



Benchmark Model: Left-Right Symmetric Model (LRSM)

$$SU(2)_L \times SU(2)_R \times U(1)_{B-L}$$

Kinetic terms of fermions $\mathcal{L} = \frac{g_R}{\sqrt{2}} (\bar{u}_R \gamma^\mu d_R) W'_\mu{}^+ + h.c.,$



$$SU(2)_L \times U(1)_Y$$

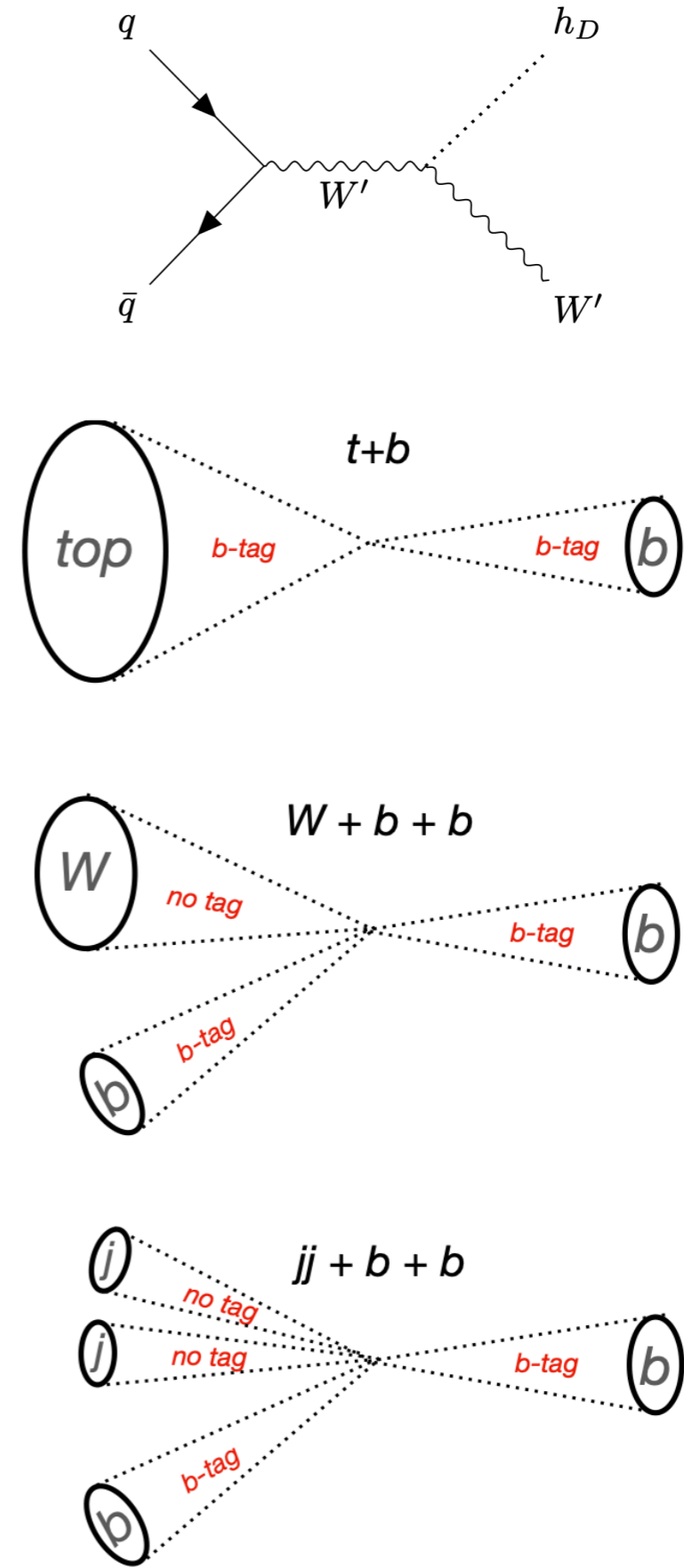
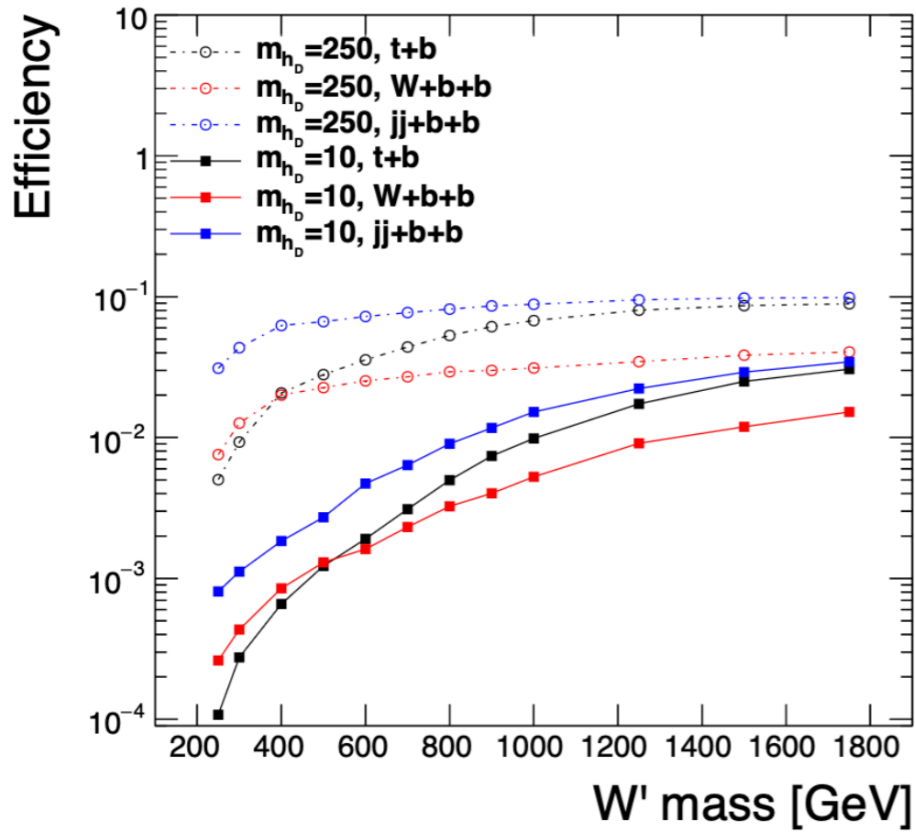
$$Q_{L,i} = \begin{pmatrix} u_L \\ d_L \end{pmatrix}_i : (\mathbf{2}, \mathbf{1}, \frac{1}{3}), \quad Q_{R,i} = \begin{pmatrix} u_R \\ d_R \end{pmatrix}_i : (\mathbf{1}, \mathbf{2}, \frac{1}{3}),$$

Kinetic terms of scalars $\mathcal{L}_{W'h_D} = g_R^2 v_R h_D (W'_\mu)^\dagger W'^\mu$

$$\begin{aligned} \Delta_R &= \begin{pmatrix} \delta_R^+/\sqrt{2} & \delta_R^{++} \\ \delta_R^0 & -\delta_R^+/\sqrt{2} \end{pmatrix} : (\mathbf{1}, \mathbf{3}, 2) \\ &= \frac{1}{\sqrt{2}} \begin{pmatrix} 0 & 0 \\ v_R & 0 \end{pmatrix} + \begin{pmatrix} \dots & \dots \\ h_D & \dots \end{pmatrix} \end{aligned}$$

g_R	$> e/c_W(0.35)$
$m_{W'}$	$\approx g_R v_R / \sqrt{2}$
m_{h_D}	Potential parameters

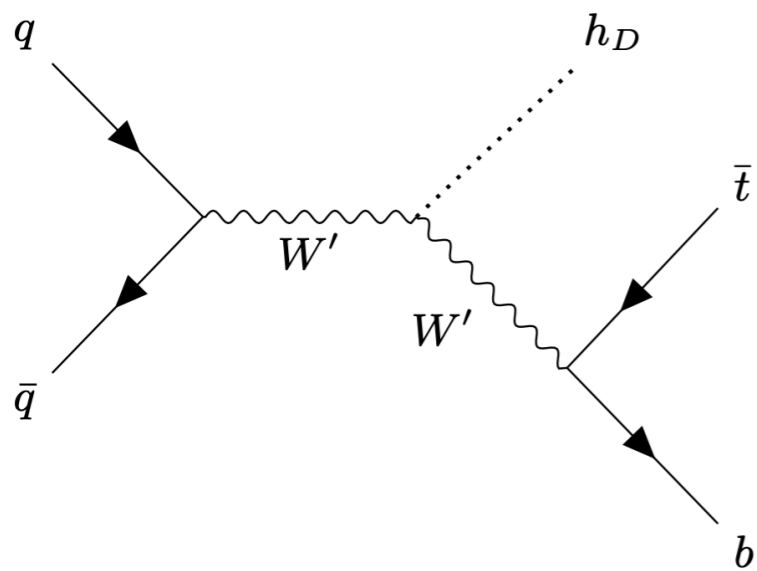
W' Candidate Reconstruction



Process	σ [fb]	ϵ	N
$t\bar{t}$	6.74×10^5	1.42×10^{-3}	2.89×10^5
$Z + b\bar{b}, Z \rightarrow \nu\nu$	2.47×10^5	1.42×10^{-4}	10560
$t\bar{b} + \bar{t}b$	1.00×10^4	2.7×10^{-4}	820
$W^\pm + b\bar{b}, W^\pm \rightarrow \ell^\pm \nu$	1.74×10^5	1.2×10^{-5}	620
$M'_W = 300, M_{h_D} = 10$	2280	0.0016	1060
$M'_W = 800, M_{h_D} = 100$	66	0.056	1120
$M'_W = 1250, M_{h_D} = 250$	16.9	0.129	650

Production cross section

The W' can be on-shell before or after emitting a dark Higgs, and these two channels have comparable contributions



2-body: $pp \rightarrow W'h_D$ then $W' \rightarrow tb$

$$\propto (g_R g_{W'W'h})^2 \quad \propto \text{constant}$$

3-body: $pp \rightarrow W'$ then $W' \rightarrow tbh_D$

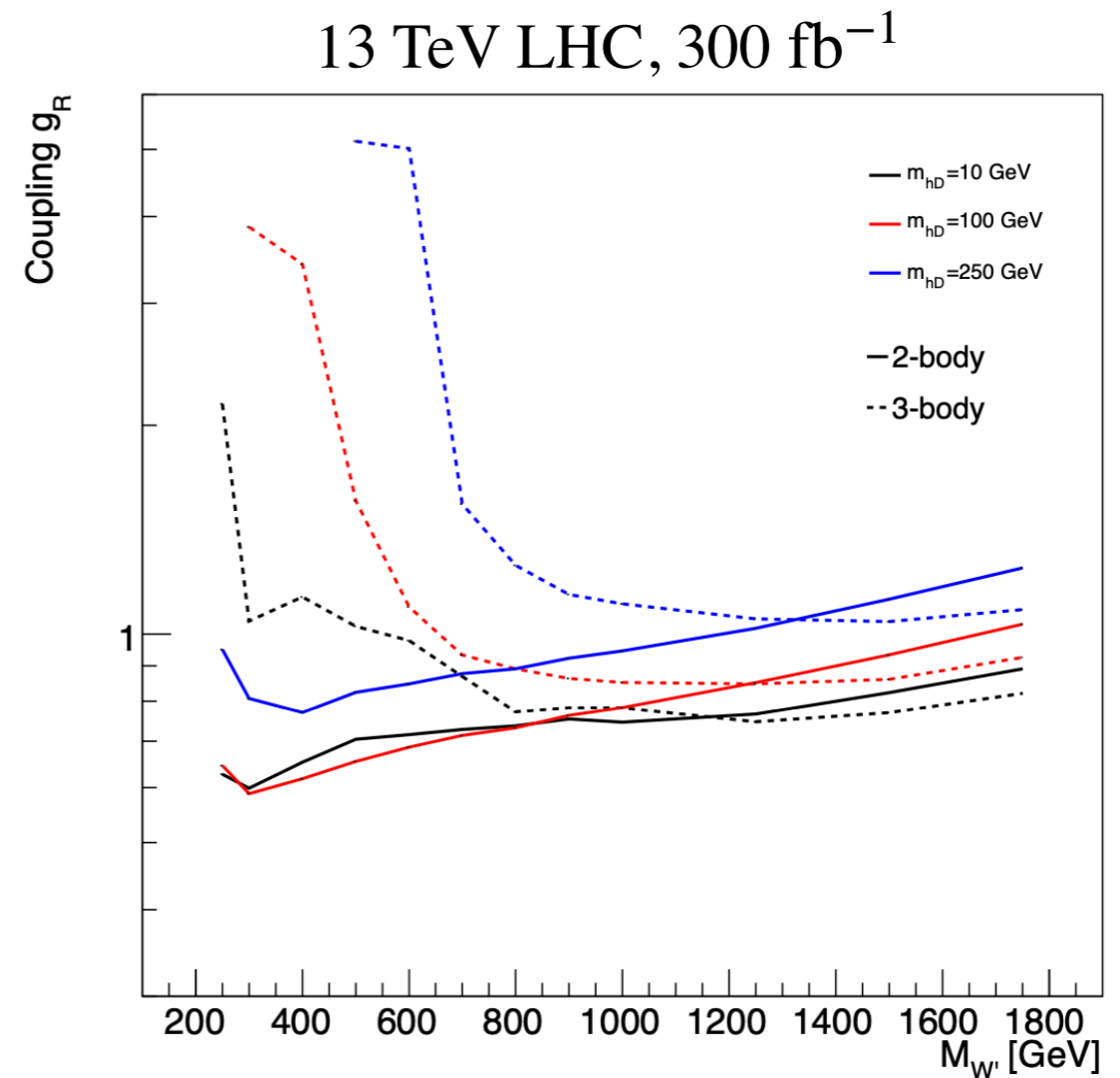
$$\propto g_R^2 \quad \propto g_{W'W'h}^2$$

We always have contribution from both channels. $\propto g_R^4$

Which cross section is larger? Only depends on the mass of W' and h_D

Results and Discussion

Current LHC data is sensitive to $W' + h_D$ production in the range of 20 fb to 30 pb. The corresponding limit on g_R can be as low as 0.6



We studied the p_T^{miss} with hadronically-decaying W' , which:

- Describes a new search mode of DM
- Expand the W' boson searches to small mass region

Backup

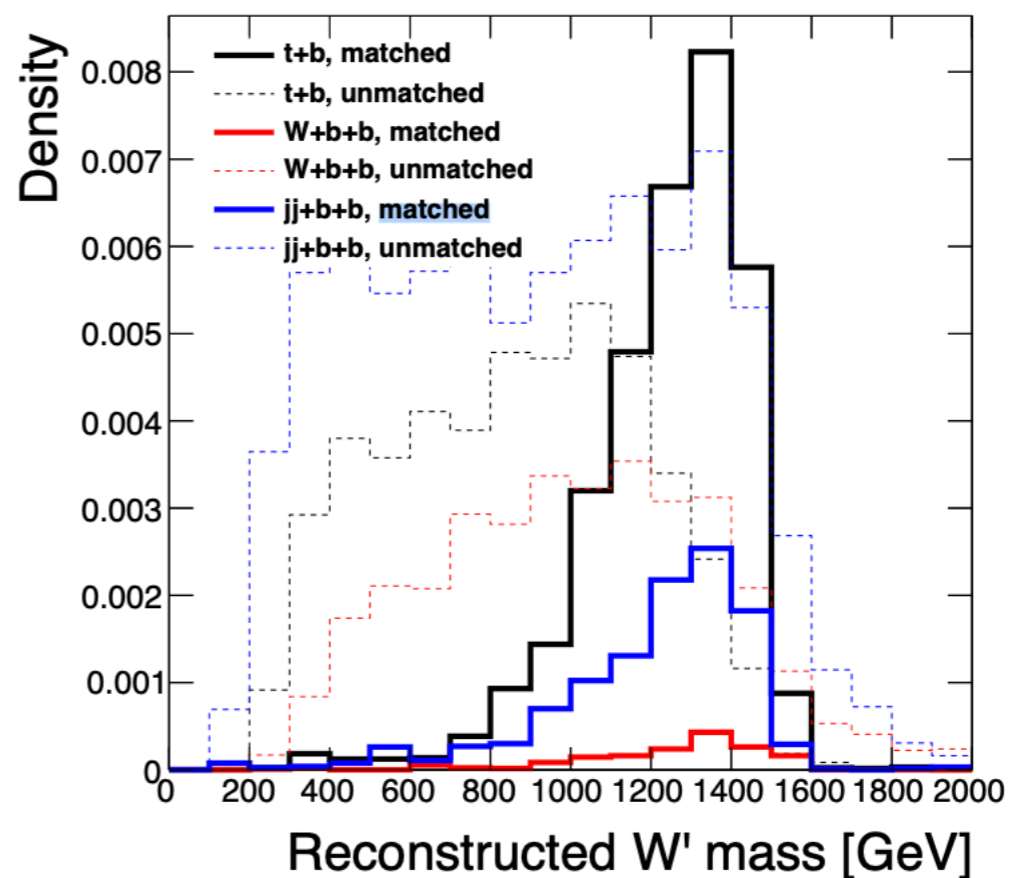
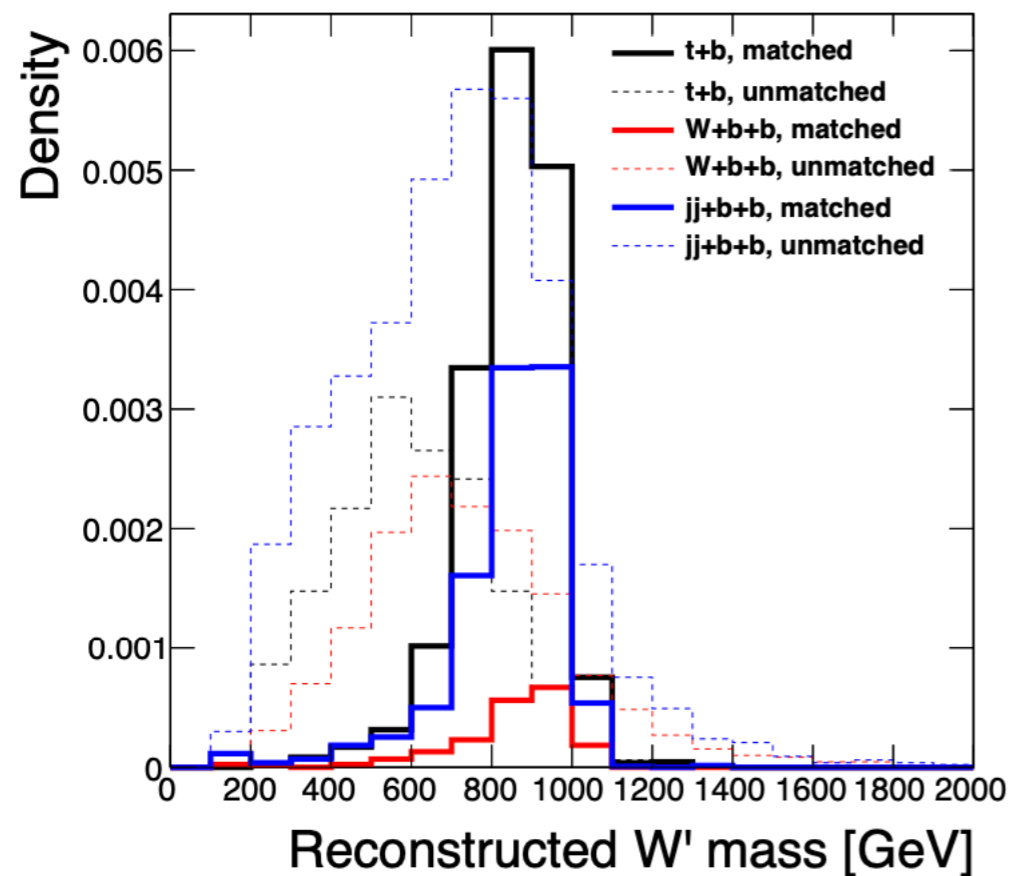


FIG. 3: Top (bottom): Distribution of the reconstructed W' boson candidate mass in simulated events with $m'_W = 1000$ (1500) GeV, for each of the three reconstruction strategies (see Fig 2), where the selected objects are angled-matched ($\Delta R < 0.4$) and -unmatched ($\Delta R > 0.4$) to the correct parton-level objects

Backup: backgrounds

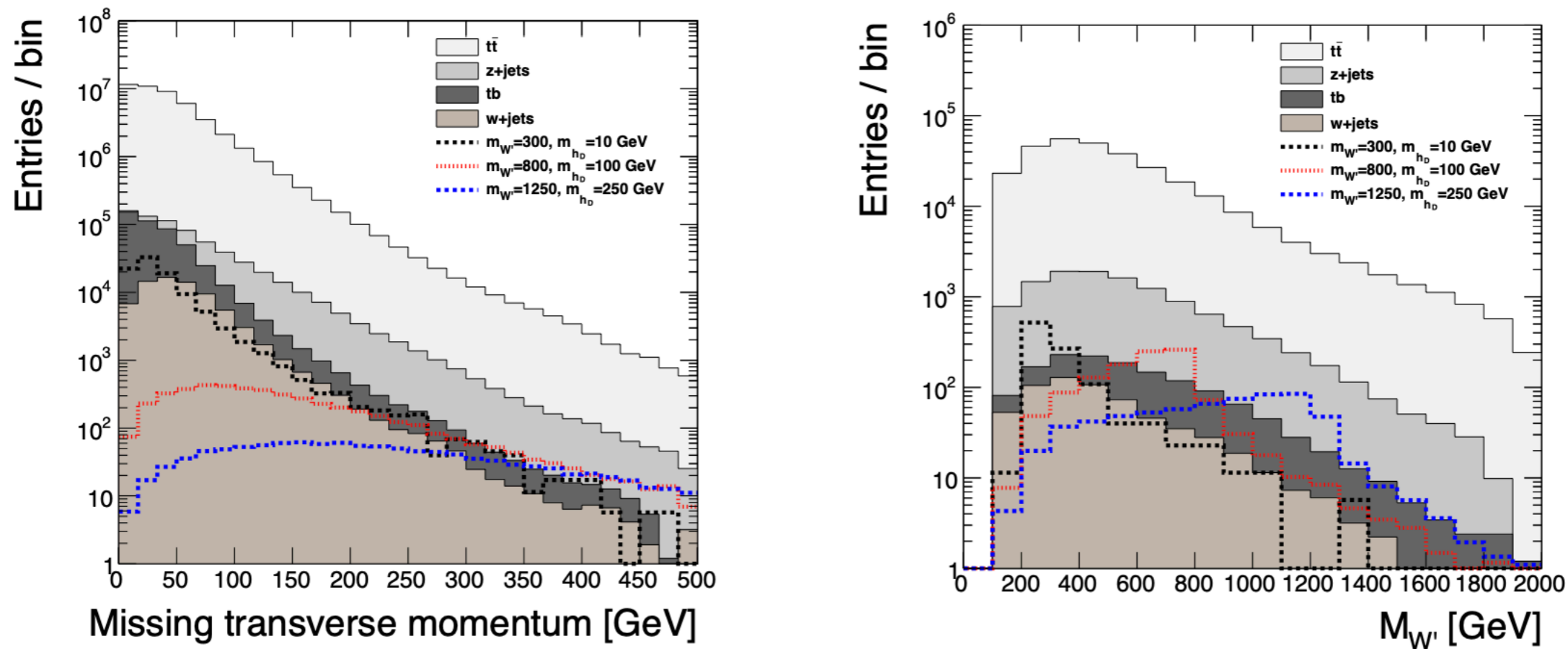


FIG. 5: Top: Distribution of the missing transverse momentum (p_T^{miss}) for the expected background and selected signals normalized to an integrated luminosity of 300 fb^{-1} after all requirements other than $p_T^{\text{miss}} > 200$ GeV are met. Bottom: Distribution of the reconstructed W' boson 2-body candidate mass for the expected background and selected signals normalized to an integrated luminosity of 300 fb^{-1} after the full selection.

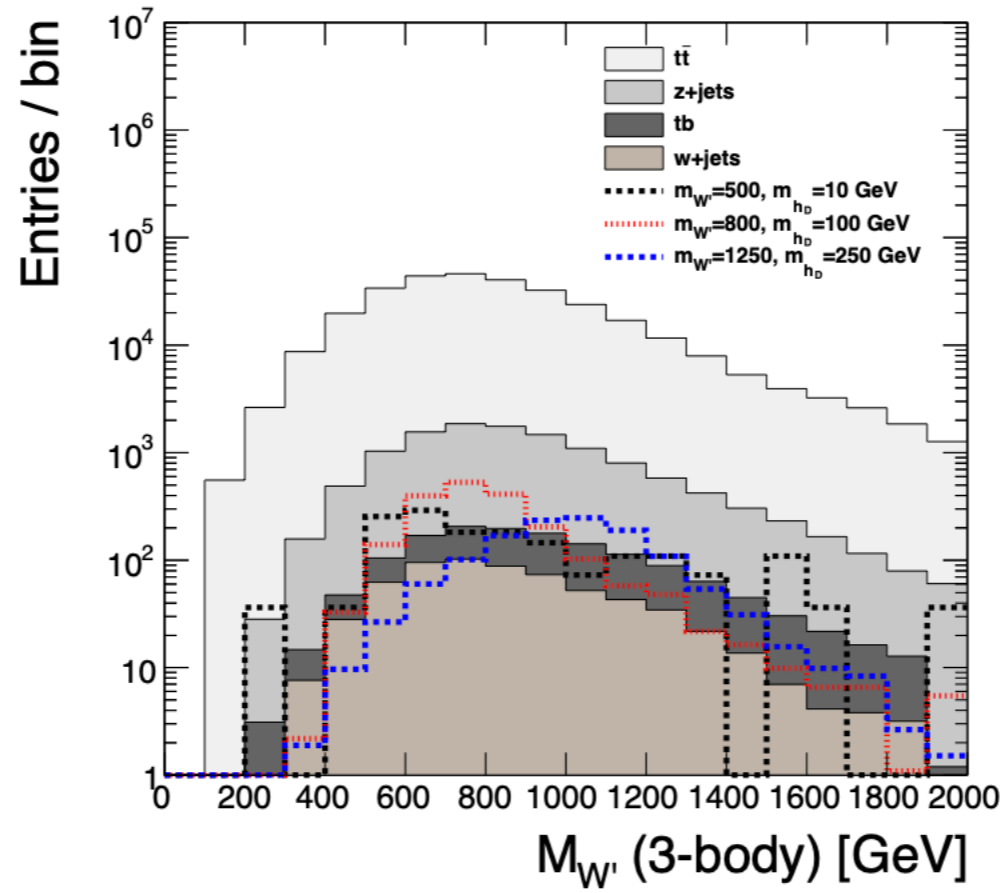


FIG. 6: Distribution of the reconstructed W' boson 3-body candidate mass for the expected background and selected signals normalized to an integrated luminosity of 300 fb^{-1} after the full selection.

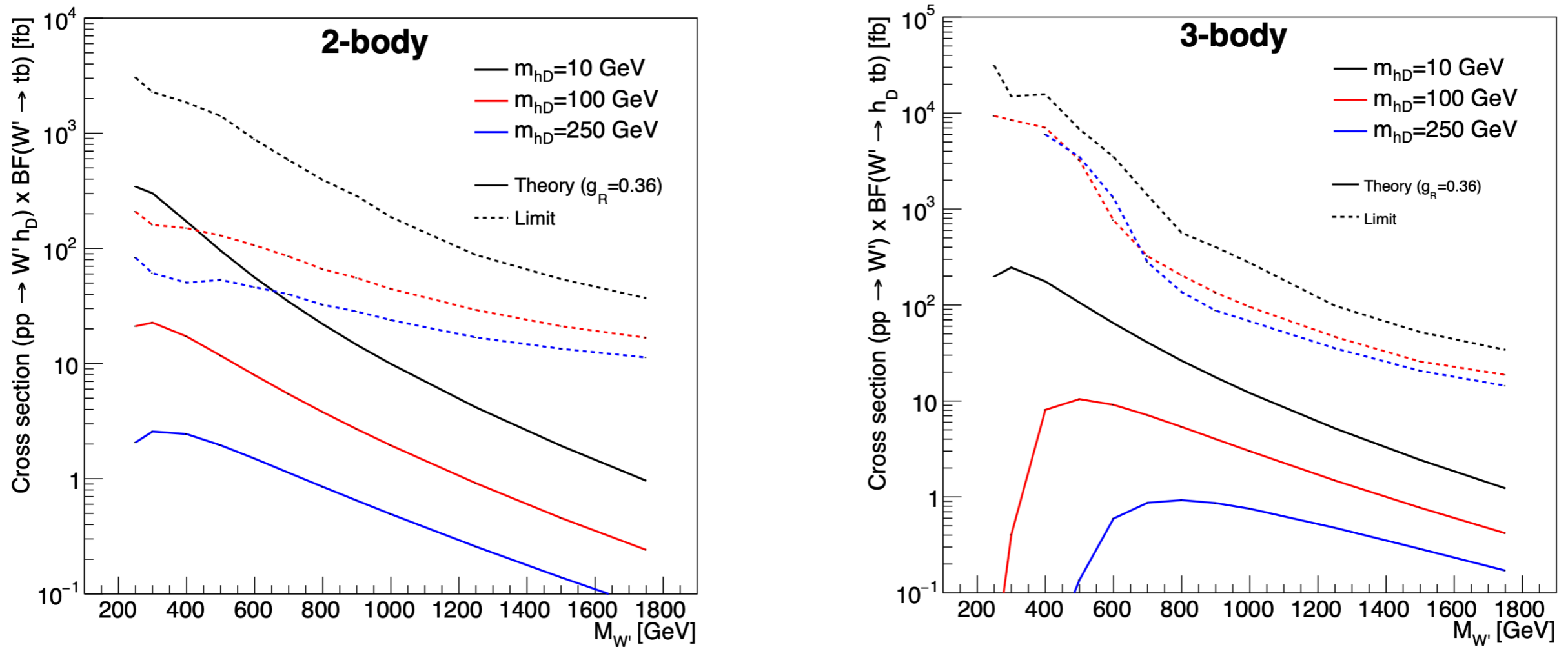


FIG. 7: Top: Summary of expected upper limits at 95% CL on the $h_D W'$ production cross section and the 2-body decay branching fraction of W' as a function of the W' boson mass normalized to an integrated luminosity of 300 fb^{-1} for three choices of the h_D boson mass. Also shown are expected theoretical cross sections and branching fractions at leading order for a coupling value of $g_R = 0.36$. Bottom: The same distributions as above except for the 3-body decay of the W' boson.